Journal of Cellular Physiology

How Dynein and Microtubules Rotate the Nucleus

JUN WU,[1] KRISTEN C. LEE,[2] RICHARD B. DICKINSON,[1]* AND TANMAY P. LELE[1]*

[1]*Department of Chemical Engineering, University of Florida, Gainesville, Florida*

[2]*Department of Biochemistry, University of Florida, Gainesville, Florida*

In living cells, a fluctuating torque is exerted on the nuclear surface but the origin of the torque is unclear. In this study, we found that the nuclear rotation angle is directionally persistent on a time scale of tens of minutes, but rotationally diffusive on longer time scales. Rotation required the activity of the microtubule motor dynein. We formulated a model based on microtubules undergoing dynamic instability, with tensional forces between a stationary centrosome and the nuclear surface mediated by dynein. Model simulations suggest that the persistence in rotation angle is due to the transient asymmetric configuration of microtubules exerting a net torque in one direction until the configuration is again randomized by dynamic instability. The model predicts that the rotational magnitude must depend on the distance between the nucleus and the centrosome. To test this prediction, rotation was quantified in patterned cells in which the cell's centrosome was close to the projected nuclear centroid. Consistent with the prediction, the angular displacement was found to decrease in these cells relative to unpatterned cells. This work provides the first mechanistic explanation for how nuclear dynein interactions with discrete microtubules emanating from a stationary centrosome cause rotational torque on the nucleus.

J. Cell. Physiol. 226: 2666–2674, 2011.

Cell and developmental processes like fertilization, cell migration, division and establishment of polarity require specific positioning of the nucleus within the cell by mechanical forces generated in the cytoskeleton (Gomes et al., 2005; Zhang et al., 2007; Jaalouk and Lammerding, 2009; Starr, 2009; Wang et al., 2009). Defects in this force-generating system are related to disorders of the nervous system (Gros-Louis et al., 2007) and the musculo-skeletal system (Jaalouk and Lammerding, 2009). Nuclear movement in the cell is a complex process that involves interactions with all three cytoskeletal systems—actin, intermediate filaments, and microtubules (Starr, 2009). On the cytoplasmic side, these interactions are mediated by molecular tethers such as nesprin family proteins that link the nuclear surface to the actin and intermediate filament cytoskeleton (Warren et al., 2005) and motor proteins such as nuclear-bound dynein that potentially generate active forces on the nuclear surface through interactions with microtubules (Levy and Holzbaur, 2008; Zhou et al., 2009; Fridolfsson et al., 2010).

Despite the importance of nuclear positioning as a critical cellular function and its relevance to disease, our understanding of how forces are generated on the nuclear surface in living cells is surprisingly limited. Typical nuclear movements observed in most cell types include translation of the nuclear centroid and the rotation of the nucleus about its axis. Nuclear translation occurs during cell crawling, but this is a considerably complicated process to study mechanistically because it is accompanied by substantial motion of the cell body (Morris, 2003; Gomes et al., 2005), associated intracellular organelles and the three cytoskeletal structures (F-actin, intermediate filaments, and microtubules). While these complicating factors are not present in the stationary cell, little nuclear translation occurs in non-moving cells. In contrast, nuclear rotation has been observed in both stationary (Yao and Ellingson, 1969; Parker et al., 2002) and translating cells (Levy and Holzbaur, 2008). The rotation of the nucleus is one mechanism by which oblong nuclei can be oriented in a migrating cell. For example, work by Levy and Holzbaur (2008) has shown that nuclear rotation is significantly increased in wounded, migrating cells and that this depends on dynein activity. Dynein-mediated pulling on the nuclear surface is crucial for nuclear positioning during cell polarization (Gomes et al., 2005) and the rotation is a quantitative readout of these forces thereby allowing the development of testable, mechanistic models for nuclear forces.

The mechanism of torque generation on the rotating nucleus has remained obscure, even though rotation has been observed in many cell types for several decades (Pomerat, 1953; Albrecht-Buehler, 1984; Allen and Kropf, 1992; Ji et al., 2007; Levy and Holzbaur, 2008). One study suggested that the rotation may be due to a transient bond between the centrosome and the nuclear membrane mediated by dynein and Hook/SUN family proteins, such that the nuclear rotation is coupled with the movement of the centrosome itself (Lee et al., 2005). A recent study showed that the migration of fibroblasts into a newly created wound triggered nuclear translocation and coupled rotation, and both were decreased in dynein-null fibroblasts (Levy and Holzbaur, 2008); interestingly these authors suggested that the centrosome is not bound to the nucleus. In non-wounded cells, another interesting feature of nuclear rotation is that the rotation angle fluctuates (Gerashchenko et al., 2009), and rotation can occur over several hours of observation (Ji et al., 2007). The cause of fluctuations and long-time persistence in the rotation angle is currently unknown.

A physical explanation for how torque could arise through interactions between nuclear bound dynein and microtubules emanating from a stationary centrosome to create fluctuating, persistent nuclear rotation is needed. In this paper, we show

Additional Supporting Information may be found in the online version of this article.

Contract grant sponsor: NSF, AHA;
Contract grant numbers: CMMI-0954302, CTS-0505929, 0735203N.

*Correspondence to: Richard B. Dickinson or Tanmay P. Lele, Department of Chemical Engineering, University of Florida, Bldg 723, Gainesville, FL 32611.
E-mail: dickinso@che.ufl.edu or tlele@che.ufl.edu

Received 15 November 2010; Accepted 15 December 2010

Published online in Wiley Online Library (wileyonlinelibrary.com), 29 December 2010.
DOI: 10.1002/jcp.22616

that in NIH 3T3 fibroblasts, nuclear rotation is a persistent random walk that requires dynein. The centrosome does not rotate with the nucleus. We formulated a model based on microtubules undergoing dynamic instability, with tensional forces between a stationary centrosome and the nuclear surface mediated by dynein. The model predicts that the fluctuations and persistence in nuclear rotation are due to the dynamic instability of microtubules. A key model prediction is that the rotation should decrease with decreasing distance between the nucleus and the centrosome. We experimentally tested this prediction by showing that rotation in patterned cells (where the centrosome overlaps with the nucleus and is close to the nuclear centroid) is considerably reduced compared to unpatterned, stationary cells with larger nuclear–centrosomal distance. Together, these results show that force generation by dynein on microtubules undergoing dynamic instability is sufficient to explain the key features of nuclear rotation.

Materials and Methods

Cell culture, plasmids, and transfection

NIH 3T3 fibroblasts were cultured in DMEM (Mediatech, Manassas, VA) with 10% donor bovine serum (Gibco, Grand Island, NY) and 1% Penn–Strep (Mediatech). For microscopy, cells were cultured on glass-bottomed dishes (MatTek Corp, Ashland, TX) coated with 5 μg/ml fibronectin at 4°C overnight.

DsRed-CC1 plasmid was kindly provided by Prof. Trina A. Schroer from Johns Hopkins University, pDsRed plasmid was kindly provided by Prof. Scott S. Grieshaber from the University of Florida. YFP-γ-tubulin was prepared from the MBA-91 AfCS Set of Subcellular Localization Markers (ATCC, Manassas, VA). Transient transfection of plasmids into NIH 3T3 fibroblasts was performed with Effectene® Transfection Reagent (Qiagen, Valencia, CA).

Time-lapse imaging and analysis

Time-lapse imaging was performed on a Nikon TE2000 inverted fluorescent microscope with a 60×/1.49NA objective and CCD camera (CoolSNAP, HQ^2, Photometrics, Tucson, AZ). During microscopy, cells were maintained at 37°C in a temperature, CO_2 and humidity controlled environmental chamber. Images were imported into MATLAB and two nucleoli in the nucleus were tracked with time to calculate the rotation angle. The positions of the nucleoli ($\vec{r}_{1j}$ and $\vec{r}_{2j}$) at time point j were calculated to sub-pixel resolution using previously published image correlation methods (Russell et al., 2009), and the angle between lines joining nucleoli in successive images was calculated as $\cos(\Delta\theta_j) = (\vec{r}_{1j}-\vec{r}_{2j})\cdot(\vec{r}_{1j+1}-\vec{r}_{2j+1})/(|\vec{r}_{1j}-\vec{r}_{2j}||\vec{r}_{1j+1}-\vec{r}_{2j+1}|)$ where $\Delta\theta_j = \theta_{j+1}-\theta_j$ is the angular displacement between time point j and j + 1. The autocorrelation function was calculated as $G_i = \sum_{j=1}^{N-i}(\Delta\theta_j)(\Delta\theta_{j+i})/(N-i)$. The mean-squared angular displacement was calculated as $MSD_j = \sum_{j=1}^{N-i}(\theta_{j+i}-\theta_j)^2/(N-i)$.

Immunofluorescence

Immunostaining studies were carried out as previously described (Chancellor et al., 2010) with mouse monoclonal anti-human γ-tubulin (Sigma, St. Louis, MO) and polyclonal rabbit anti-human α-tubulin (Abcam, Cambridge, MA) antibodies, and Hoechst 33342 in 4% paraformaldehyde fixed cells permeabilized with 0.1% Triton X-100 in PBS. Goat anti-mouse and goat anti-rabbit antibodies conjugated with Alexa Fluor 488 and Alexa Fluor 594 fluorescent dyes (Invitrogen, Carlsbad, CA) were used as secondary antibodies.

Cell shape patterning

Cell shape patterning was done by using the microcontact printing technique described in Fink et al. (2007). Molds for the stamps were produced with the UV lithography technique by illuminating a positive photoresist through a chrome photomask on which micropatterns were designed (Photo Sciences, Inc., Torrance, CA). PDMS (Sylgard 184 kit, Dow Corning, Midland, MI) was cast on the resist mold using a 10:1 ratio (w/w) of elastomer to hardener and cured at 60°C for 2 h and postcured at 100°C for 1 h. For micropatterning, the PDMS stamp was treated with 50 μg/ml human fibronectin solution (BD Biocoat™, Franklin Lakes, NJ). The stamp was then dried and placed onto the substrate onto which the cells were plated. Ibidi dishes (Ibidi, Verona, WI) were chosen as the substrate. After 5 min, the stamp was removed and the remaining area was blocked with PLL-g-Poly-ethylene glycol (SuSoS AG, Dübendorf, Switzerland), preventing protein adsorption and cell attachment. After treatment the surface was washed and cells were plated.

Results

Nuclear rotation is a persistent random walk

Nuclear rotation has been typically studied by time-lapse microscopy; however, a quantitative analysis of fluctuating nuclear rotation has not been previously reported. We measured nuclear rotation angle with high accuracy using image correlation methods. The nucleus (and its contents) is known to rotate as a solid object (Paddock and Albrecht-Buehler, 1988), therefore tracking fiduciary markers on the nucleus (nucleoli) allowed us to calculate the angular displacement between successive images. By tracking the non-moving nucleus in cells fixed with paraformaldehyde which cross-links the cellular contents and ensures zero rotation, we calculated the error in the image correlation as being less than 1%. As shown by the trajectories in Figure 1, the net angle through which the nucleus rotates exhibited short-time fluctuations and typically long-time persistence in the direction of rotation. Most trajectories displayed a significant angle of rotation in around 2 h, while some fluctuated in position without achieving much net displacement.

To quantitatively characterize the angular trajectories, the average mean-squared angular displacement (MSD) was estimated (see Materials and Methods Section for how MSD was calculated) from data pooled from several cells (Fig. 1C). The MSD showed characteristics of a persistent random walk, with a parabolic shape at short time approaching linearity at long time (Fig. 1C). To further characterize the directional persistence, we estimated the autocorrelation function of angular displacements (Fig. 1C, inset). This autocorrelation function resembled a double exponential, reflecting the relaxation of short-time fluctuations in directional rotation and longer-time relaxation of persistent directional rotation.

Cytoplasmic dynein is required for nuclear rotation in stationary fibroblasts

To determine the role of dynein in nuclear rotation in stationary fibroblasts, we transfected cells with DsRed-CC1, which inhibits dynein by competitive binding (Quintyne et al., 1999; King et al., 2003). pDsRed plasmid transfected cells were used as the control. Transfection with DsRed-CC1 significantly decreased nuclear rotation compared with cells expressed the control pDsRed plasmid (Fig. 2). We also found that rotation was abolished upon depolymerizing microtubules (Fig. S1 in Supplementary Material). Also, the centrosome was observed not to rotate with the nucleus, but rather occupied a relatively fixed position in space even as the nucleus rotated through a significant angle (see Movies S1, S2 and Fig. S2). These results are consistent with recent observations by Levy and Holzbaur (2008) in wounded fibroblasts, and Gerashchenko et al. (2009) in non-wounded murine cells.

Model formulation

We developed a mechanistic model for dynein forces on the nucleus. The purpose of this model is to demonstrate that

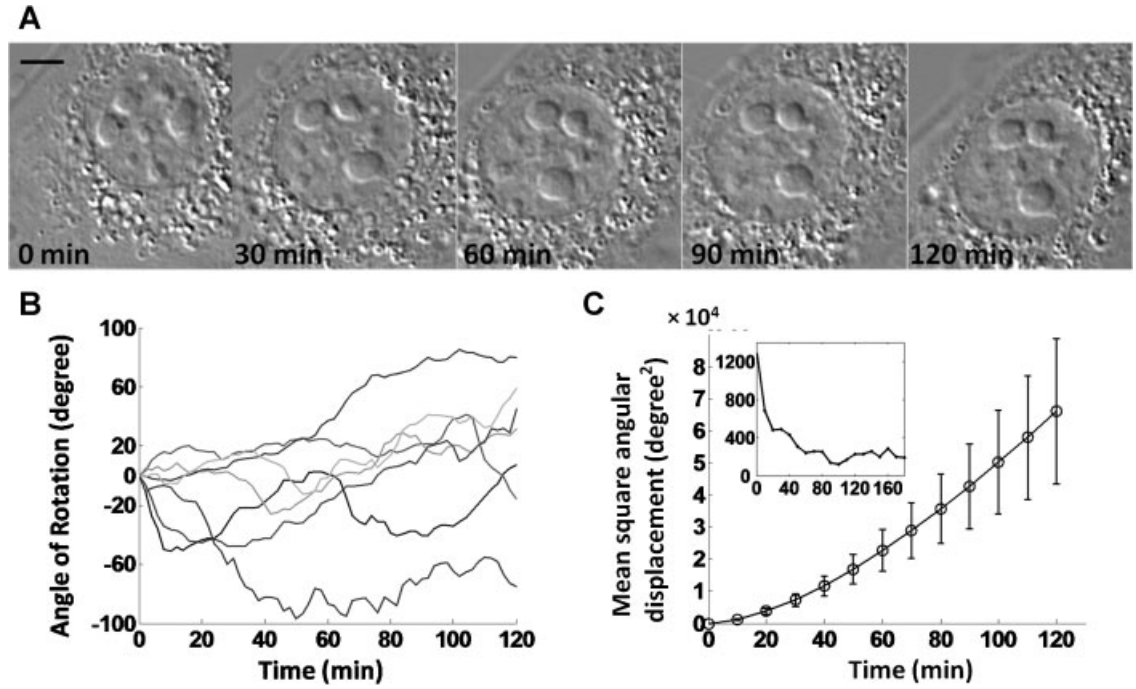

Fig. 1. Nuclear rotation is a biased random walk in NIH 3T3 fibroblasts. A: Captured images of a rotating nucleus. Scale bar is 5 μm. B: Plot shows measured trajectories of nuclear rotation; each trajectory corresponds to a single cell; only a few trajectories are shown for clarity. Time dependence of the rotation angle; time between successive data points is two minutes. The angle fluctuates randomly. C: Time-dependence of the pooled angular mean-squared displacement (n = 25 cells). The MSD shows a parabolic shape at short times followed by a linear dependence at longer times which indicates a persistent random walk. Inset shows the averaged autocorrelation of angular displacements over 10-min intervals (degree^2/min^2) indicating a fast decay followed by long time decay, again consistent with the conclusion that the rotation is a persistent random walk. Error bars indicate standard error (SE).

retrograde MT-associated motors pulling on the nucleus are sufficient to explain nuclear rotation with observed statistical characteristics. Individual dynein molecules on MTs within a range σ of the nucleus are assumed to transiently bind and pull the nucleus toward the microtubule (−)-ends (Fig. 3). As is typically assumed for molecular motors, the motor speed v_m depends on the pulling force **f** (a vector) that the dynein molecule exerts on the nucleus. For simplicity, the force-speed relation for dynein motors is assumed approximately linear (Toba et al., 2006), similar to other recent studies on dynein-mediated nuclear translation (Vogel et al., 2009)

$$\frac{v_m}{v_{max}} = 1 + \frac{\mathbf{n}\cdot\mathbf{f}}{f_{max}} \tag{1}$$

where **n** is a unit vector directed toward the (+)-end of the MT. Here, v_{max} represents the speed at zero load and f_{max} represents the stall force required of the motor, such that the motor stalls when the component of the pulling force in the (−)-end direction is equal to f_{max}.

MT–nucleus linkages are assumed to have a finite lifetime, such that the force accumulated by translation of the nuclear surface at velocity **v** relative to the MT (assumed stationary), or by the motor walking along the MT, is relieved upon dissociation of the linkage. The accumulation of the force depends on the stiffness of the linkage, and it is simplest to assume that the linkages behave as linear springs with stiffness κ. Thus, accounting for the changing load, the force on the nuclear surface changes with time t, as

$$\frac{d\mathbf{f}}{dt} = -\kappa(\mathbf{v} + v_m\mathbf{n}) \tag{2}$$

Upon substitution of Equation (1) for v_m and integration, this becomes

$$\mathbf{f}(t) = -f_{max}\left(1 + \frac{\mathbf{n}\cdot\mathbf{v}}{v_{max}}\right)\left\{1 - \exp\left[-\frac{\kappa v_{max}}{f_{max}}t\right]\right\}\mathbf{n} - \kappa(\mathbf{v} - (\mathbf{n}\cdot\mathbf{v})\mathbf{n})t \tag{3}$$

Linkages are assumed to dissociate with a first-order rate constant k_{off} (sec^{-1}) such that the probability of a linkage existing at time t is $P_b(t) = e^{-k_{off}t}$. The mean force over the bond lifetime η is thus

$$\langle \mathbf{f} \rangle = -\int_0^\infty f(\eta)dP_b(\eta) = -f_0\left(1 + \frac{\mathbf{n}\cdot\mathbf{v}}{v_{max}}\right)\mathbf{n} - \frac{\kappa}{k_{off}}(\mathbf{I} - \mathbf{nn})\mathbf{v} \tag{4}$$

where $f_0 \equiv f_{max}/((f_{max}k_{off})/(\kappa v_{max}) + 1)$ is the average force per dynein molecule on a stationary nucleus. For dynein density (number/length) ρ, the net mean force per unit length, **K**, is then

$$\mathbf{K} = -F_0\left(1 + \frac{\mathbf{n}\cdot\mathbf{v}}{v_{max}}\right)\mathbf{n} - \gamma(\mathbf{I} - \mathbf{nn})\mathbf{v} \tag{5}$$

where $F_0 \equiv \rho f_0$ is the mean longitudinal force/MT length for a stationary nucleus, and $\gamma \equiv \rho\kappa/k_{off}$ is the friction coefficient ((force/speed)/MT length) to lateral motion.

Mechanics and kinematics of the nucleus. The net force and torque exerted on the nucleus by an MT depends on

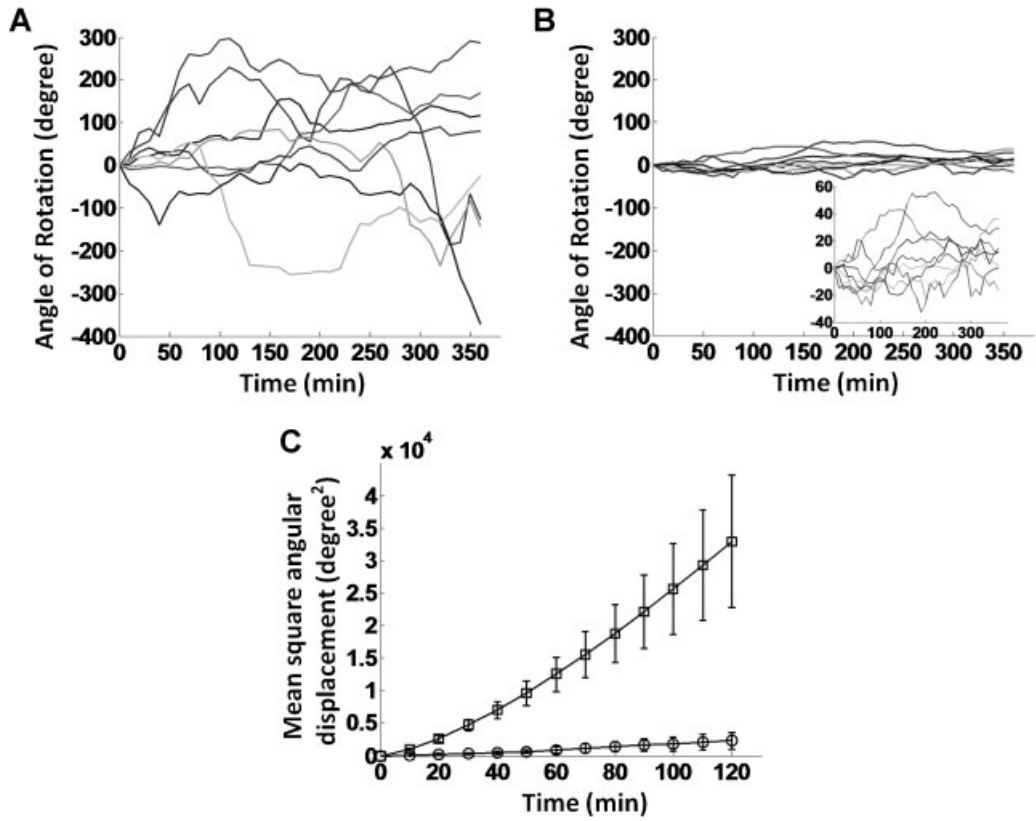

Fig. 2. Dynein inhibition significantly reduces nuclear rotation. NIH 3T3 fibroblasts were transfected with pDsRed as mock control (A), and pDsRed-CC1 for dynein inhibition (B; inset is re-scaled plot, only a few trajectories are shown for clarity). A clear decrease in the rotation is observed in dynein inhibited cells. This is confirmed from the MSD plots (C), with MSD in control cells (squares, n = 14 cells) found to be significantly larger than that in dynein inhibited cells (circles, n = 11 cells). Error bars indicate SE.

the length span of the MT that is close enough to interact with the nucleus. Let **n**s be the position vector on the MT parameterized by contour length s, between the centrosome position ($s = 0$) and the (+)-end ($s = s_{end}$). Further, let s_1 and s_2 represent the beginning and end of the interaction range with the nucleus in which the distance between the MT and nuclear surface is within σ. Based on the geometry of a line passing near a sphere, MT will interact with the nucleus provided $(R+\sigma)^2 > (\mathbf{r}_0{}^2 - (\mathbf{n}\cdot\mathbf{r}_0)^2)$ where r_0 is the center of rotation of the nucleus. The endpoints of the interacting span of the MT are then

$$s_1 = \max\left\{0, \mathbf{n}\cdot\mathbf{r}_0 - \sqrt{(R+\sigma)^2 - (\mathbf{r}_0{}^2 - (\mathbf{n}\cdot\mathbf{r}_0)^2)}\right\},$$
$$s_2 = \min\left\{s_{end}, \mathbf{n}\cdot\mathbf{r}_0 + \sqrt{(R+\sigma)^2 - (\mathbf{r}_0{}^2 - (\mathbf{n}\cdot\mathbf{r}_0)^2)}\right\} \quad (6)$$

where s_{end} is the contour position of the (+)-end. The net MT force and torque are thus

$$\mathbf{F} = \int_{s_1}^{s_2} \mathbf{K}\,ds = -\rho \int_{s_1}^{s_2} \left\{ f_0 \left(1 - \frac{\kappa}{k_{off} f_{max}} \mathbf{n}\cdot\mathbf{v}(s)\right)\mathbf{n} - \frac{\kappa}{k_{off}}\mathbf{v}(s)\right\} ds \quad (7)$$

$$\tau = \int_{s_1}^{s_2} (\mathbf{n}s - \mathbf{r}_0) \times \mathbf{K}\,ds = -\rho \int_{s_1}^{s_2} \left\{ f_0 \left(1 - \frac{\kappa}{k_{off} f_{max}} \mathbf{n}\cdot\mathbf{v}(s)\right) (\mathbf{n}\times\mathbf{r}_0) - \frac{\kappa}{k_{off}} (\mathbf{n}s - \mathbf{r}_0)\times\mathbf{v}(s)\right\} ds \quad (8)$$

where the local velocity **v** generally depends on translation and rotation as

$$\mathbf{v}(s) = \mathbf{V}_{nuc} + \omega_{nuc} \times (\mathbf{n}s - \mathbf{r}_0) \quad (9)$$

Neglecting other cytoskeletal (frictional) contributions to force and torque on the nucleus and neglecting inertia, the net force and torque balances are

$$\sum_i \mathbf{F}_i = 0 \quad (10)$$

$$\sum_i \tau_i = 0 \quad (11)$$

which yield six equations for the six unknown components of vectors **v** and ω.

The model can be simplified substantially by neglecting translation (assuming that the distance between the centrosome and the nucleus does not change during rotation;

see Figure S2 in Supplementary Information) and allowing rotation only about the vertical z-axis, consistent with experimental observations. A possible explanation for rotation about only the z-axis is that the nucleus is compressed into an oblate spheroid by cell spreading (Khatau et al., 2009; Chancellor et al., 2010), thus rotation in other directions is resisted as it requires substantially more deformation of the cytoskeleton. Hence, rather than six degrees of freedom, we need only consider the component of the rotational velocity normal to the image plane ($\omega_{nuc,z}$) determined by solving $\sum_i \tau_{z,i} = 0$ such that

$$\omega_z = \frac{-\frac{f_0 k_{off}}{\kappa}\sum_i \rho_i (r_{0,x}n_{y,i} - r_{0,y}n_{x,i})(s_{2,i} - s_{1,i})}{\sum_i \rho_i \left\{\frac{f_0}{f_{max}}(r_{0,x}n_{y,i} - r_{0,y}n_{x,i})(s_{2,i} - s_{1,i}) + \frac{1}{3}(n_{x,i}^2 + n_{y,i}^2)(s_{2,i}^3 - s_{1,i}^3) - (n_{x,i}r_{0,x} + n_{y,i}r_{0,y})(s_{2,i}^2 - s_{1,i}^2) + (r_{0,x}^2 + r_{0,y}^2)(s_{2,i} - s_{1,i})\right\}} \quad (12)$$

Lastly, although dynein may uniformly coat the nuclear surface, we speculate that linkages are most readily formed when MTs run parallel to the nuclear surface and are inhibited when MTs impinge normal to the surface. To account for this, we assume that the effective local linkage density $\rho_i = \rho \sin\phi_i$ varies with angle of incidence ϕ_i of the MT with the surface as $\rho_i = \rho \sin\phi_i$. Upon canceling ρ from numerator and denominator, Equation (12) becomes

$$\omega_z = \frac{-\frac{f_0 k_{off}}{\kappa}\sum_i \sin\phi_i (r_{0,x}n_{y,i} - r_{0,y}n_{x,i})(s_{2,i} - s_{1,i})}{\sum_i \sin\phi_i \left\{\frac{f_0}{f_{max}}(r_{0,x}n_{y,i} - r_{0,y}n_{x,i})(s_{2,i} - s_{1,i}) + \frac{1}{3}(n_{x,i}^2 + n_{y,i}^2)(s_{2,i}^3 - s_{1,i}^3) - (n_{x,i}r_{0,x} + n_{y,i}r_{0,y})(s_{2,i}^2 - s_{1,i}^2) + (r_{0,x}^2 + r_{0,y}^2)(s_{2,i} - s_{1,i})\right\}} \quad (13)$$

Simulations of dynamic instability and nuclear rotation. The rotational velocity obtained from Equation (13) depends on the current configuration of microtubules. In the simulations, MTs are assumed to elongate at constant speed V_{pol} from the centrosome until catastrophe occurs. When catastrophe occurs, MTs begin to shrink at a constant speed V_{depol} until recovery. On recovery, they begin to grow again. Catastrophe and recovery have constant probabilities per unit time k_{cat} and k_{rec} respectively. The parameters are shown in Table 1. If an MT shrinks completely to the centrosome, a new MT immediately nucleates in another random direction on the unit sphere thereby maintaining a constant number N of MTs. Any MT which impinges on the cell or nuclear boundaries is assumed to stop growing and remain a constant length until catastrophe. MTs are assumed straight and rigid in this treatment. Although actual MTs are not straight in vivo, MTs typically do not change much in direction over the distance from the centrosome to the nucleus; therefore treating them as straight is a reasonable simplification. Another complication is that some MTs may wrap-trace along the nuclear surface, thereby increasing the effective interaction length of the MT. However, increasing the span of interaction is similar to changing the dynein density, which has no effect on the predicted long-time dynamics. This is because changing the interaction span changes both the pulling force and opposing friction force by equal proportions (see Equation 13 which shows that the rotational velocity does not depend on ρ, the density of dynein).

Model results

We hypothesized that the rotation was due to an imbalance of torque from MT-associated dynein pulling forces on the nucleus. In this model, an instantaneous imbalance in the net dynein pulling force would arise when, as the MT configuration evolves due to dynamic instability, more microtubules contact one side of the nucleus than the other. Angular trajectories simulated based on this model reproduced motions that were qualitatively similar to those observed experimentally (Fig. 4A,B and Movies S3 and S4). Like the experimental data, the autocorrelation function of the simulated trajectories exhibited short-time fluctuations due to stochastic contacts between the MTs and the nucleus, and a long-time directional persistence in rotation that relaxed as the MT network relaxed due to dynamic instability (Fig. 4C), as evident by the long-time non-zero tail of the autocorrelation plot. The time scale of the fluctuations, which is evident in the autocorrelation function of 10 min displacements, depends primarily on the parameter group κ/k_{off} of which a value of 56 pN-sec/μm yielded good quantitative agreement to the experimental data. This value also yielded excellent agreement for the mean-squared displacement (Fig. 4D). Based on recent FRAP measurements of cytoplasmic dynein (Yamada et al., 2010), a rough estimate of $k_{off} \sim 0.02$ sec^{-1}. Then $\kappa \sim 1$ pN/μm, which is not unreasonable for proteins (Howard, 2006).

A testable prediction of this model is that the amount of rotation caused by an anisotropic configuration of MTs should decrease when the centrosome directly underlies the nucleus. As shown in Figure 4E, the mean-squared rotation angle measured from the simulations decreased as the centrosome was placed at positions closer to the nuclear centroid. This prediction can be explained by the fact that the dynein-generated torque is smaller when the lever arm length (i.e., the distance from the nuclear centroid to the MT–nucleus contact position) is smaller (Fig. 3B). We tested this model prediction by patterning cells into symmetrical shapes as discussed below.

Nuclear rotation depends on nuclear–centrosomal distance

In stationary, unpatterned cells, the centrosome is typically observed in two-dimensional images at one side of the nucleus (Fig. 5A), and below the mid-plane of the nucleus. It is known that the centrosome is positioned at the cell centroid due to centering by dynamic microtubules interacting with the cell periphery (Burakov et al., 2003). We reasoned that in patterned cells of square shape, the centrosome should be located at the

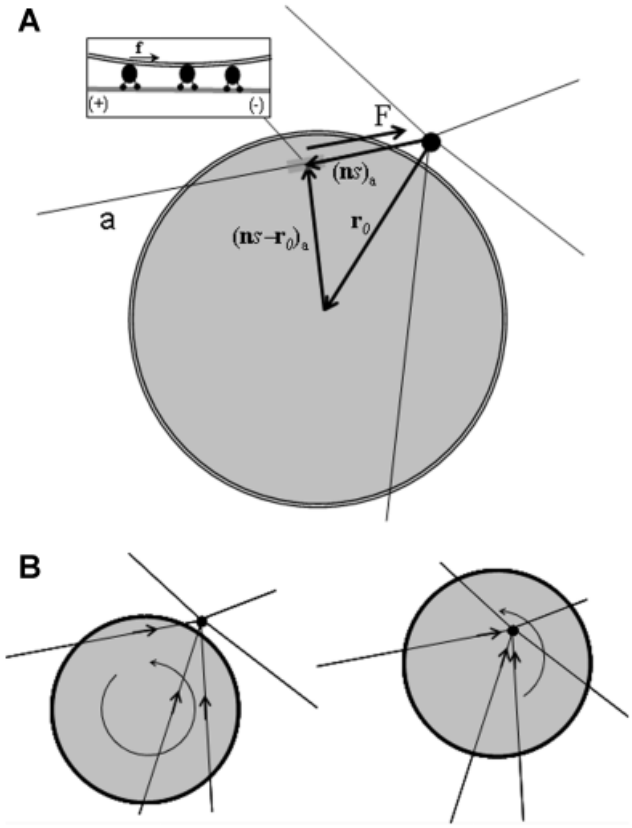

Fig. 3. Schematic of the nuclear rotation model. A: Dynein molecules walking on microtubules (straight lines) generate forces (f) on the nuclear surface directed toward the centrosome (intersection of straight lines). The resulting mean net force F from the microtubule and the lever arm (vector $ns - r_0$ where s is the position on the contour, n is a unit vector directed toward the MT plus-end, and r_0 is a unit vector directed from the centrosome to the center of the nucleus) create a torque on the nucleus. B: The magnitude of the torque depends on the centrosome position, because the lever arm length is smaller when the centrosome is closer to the nucleus centroid.

geometrical center of the square; this was indeed found to be the case (Fig. 5A). The nucleus was also observed close to the center of the square, such that the centrosome overlapped with the nucleus in two-dimensional images (Fig. 5A). Confocal imaging showed that the centrosome was underneath the nucleus in patterned cells (Fig. S3). This arrangement was rarely observed in unpatterned cells; the projected distance between the centrosome and the nuclear centroid was significantly higher in unpatterned cells (Fig. 5B,C).

Our model predicts that a decrease in nuclear–centrosomal distance should result in decreased torque on the nucleus for a given MT configuration. To test this prediction, we tracked rotation of the nucleus in square cells. The nucleus in square cells was observed to rotate significantly less than unpatterned cells (Fig. 6), confirming a key prediction of the model. Indeed, as indicated by the solid lines in Figure 6, the MSD generated by simulations performed with the centrosome located at the experimentally measured average position in patterned cells agreed quantitatively with experimental measurements.

Discussion

In this paper, we quantified the persistent directional rotation of cell nuclei in fibroblasts and used the data to propose a mechanistic model that can predict nuclear motion based on tensional forces on perinuclear microtubules generated by the minus ended motor dynein. In this model, the mean force per dynein molecule depends on the local velocity of the nucleus relative to the microtubule, and the net force and torque on the nucleus depends on the instantaneous configuration of perinuclear microtubules. The model qualitatively captures the dynamic behavior of nuclear rotation, and agrees quantitatively upon fixing one unknown parameter group (κ/k_{off}). We experimentally tested a key prediction of the model that the rotation should depend on the nuclear–centrosomal distance. Together, this work provides the first mechanistic explanation for how nuclear dynein interactions with discrete microtubules emanating from a stationary centrosome can cause nuclear rotation.

The finding that the centrosome is close to the nuclear centroid in patterned cells can be explained by the nearly isotropic inward flow of actomyosin from the cell periphery (Thery et al., 2006). As rearward flow continuously occurs from the corners of the squares of the patterned cells (Brock and Ingber, 2005), "equal" forces are exerted by rearward flow of actin which causes the nucleus to be centered (although not perfectly depending on the local shape of the lamellipodial protrusions). Because the centrosome is centered at the cell centroid due to microtubule–cortical actin interactions mediated by dynein (Burakov et al., 2003), this forces the nucleus and the centrosome to overlap. In unpatterned cells, the centrosome is always observed on one side of the nucleus, probably due to asymmetrical positioning of the nucleus by rearward actin flow only from the leading edge of the (polarized) cell.

The decrease in nuclear rotation in patterned cells can be interpreted in the light of the model shown in Figure 3. When the centrosome is under the nucleus, then torque is generated primarily by microtubules oriented parallel to the lower nuclear surface. When the centrosome is not underneath the nucleus but rather to the side, then the net torque generated is expected to be higher when the MT configuration evolves by dynamic instability to become spontaneously asymmetric. Mathematically, the z-component of the torque decreases to

TABLE 1. Model parameters

Symbol	Parameter	Range	Source	Value used
f_{max}	Maximum dynein force	5–8 pN	Gennerich et al. (2007)	7 pN
v_0	Speed of unstressed dynein	0.8 μm/sec	Toba et al. (2006)	0.7 μm/sec
κ	Dynein spring constant	No measured value		$\kappa/k_{off} = 56$ pN-sec/μm
k_{off}	Dynein–nucleus off-rate	No measured value		
ρ	Dynein density (number/length)	No measured value		Not needed
N	Number of microtubules	200–500	Gliksman et al. (1993)	250
V_{pol}	MT polymerization speed	5–10 μm/min	Gliksman et al. (1993) and Shelden and Wadsworth (1993)	7 μm/min
V_{depol}	MT depolymerization speed	15–20 μm/min	Gliksman et al. (1993) and Shelden and Wadsworth (1993)	17 μm/min
k_{cat}	MT catastrophe rate constant	0.01–0.06 sec^{-1}	Gliksman et al. (1993) and Shelden and Wadsworth (1993)	0.05 sec^{-1}
k_{rec}	MT recovery rate constant	0.04–0.2 sec^{-1}	Gliksman et al. (1993) and Shelden and Wadsworth (1993)	0.19 sec^{-1}
σ	MT–nucleus interaction distance		Based on length of cytoplasmic dynein	60 nm

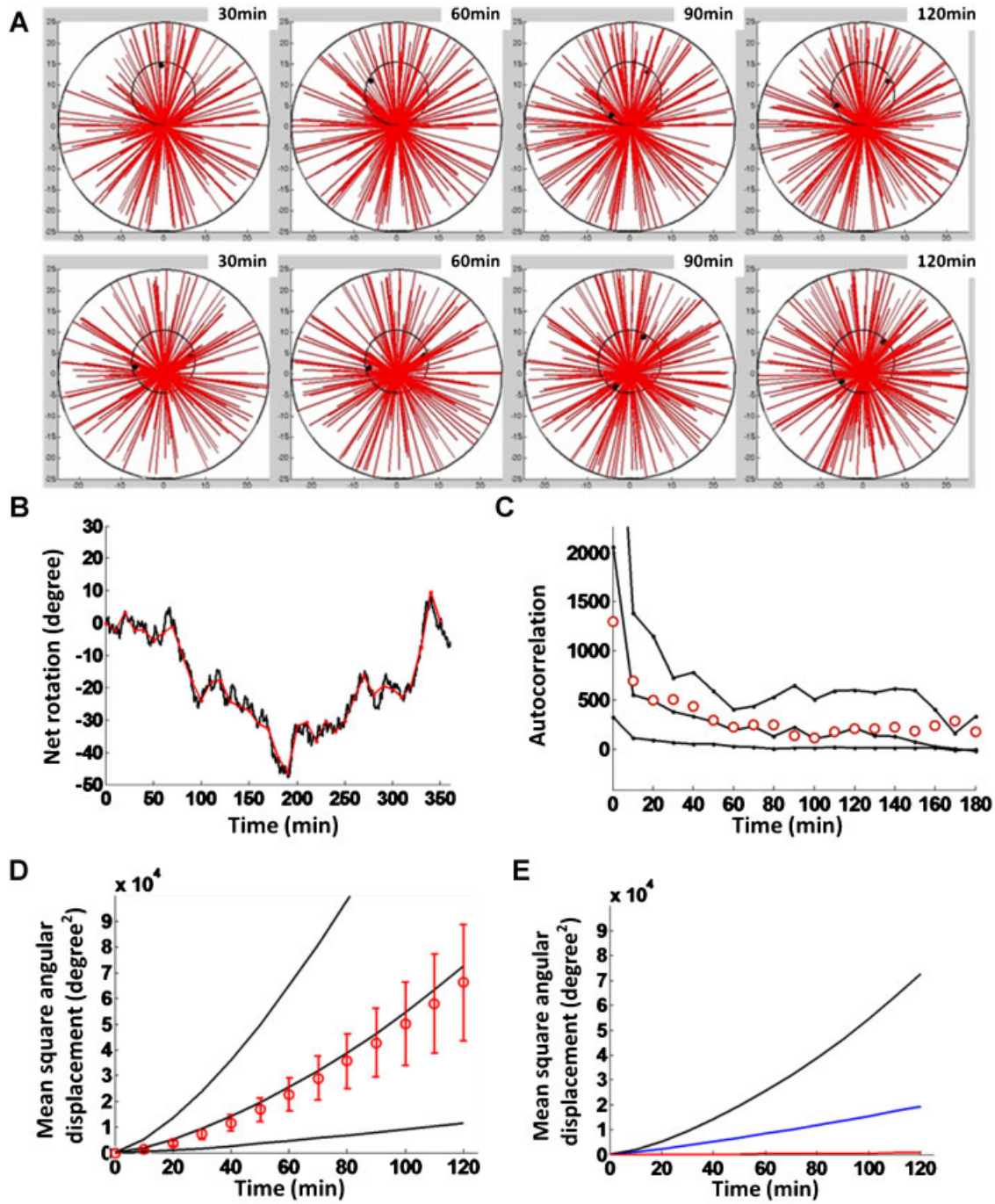

Fig. 4. Simulations of nuclear rotation in a circular cell. A: Simulation snapshots of microtubule configuration and nucleus orientation at 30-min intervals, for two different centrosome positions: A distance of 8 μm from the nucleus center (upper sequence), and a distance of 3 μm from nucleus center (lower sequence). Diameter of the cell is 50 μm. B: Example simulation trajectory of nuclear rotation (default parameters are shown in Table I), exhibiting short-term fluctuations and long-time directional persistence. The same trajectory sampled at 10-min intervals (red, as done in the experiments) is also shown. C: The autocorrelation function of rotational displacements is plotted versus time increment (solid lines), as calculated by the same method used for Figure 1C (inset), for three values of κ/k_{off} (from upper to lower: $\kappa/k_{off} = 20$, 55, and 200 pN-sec/μm, respectively. Red circles indicate the calculated average autocorrelation function from experimental trajectories. D: Model predictions of mean-squared angular displacement versus time for the same parameters in (C) (solid lines, from upper to lower: $\kappa/k_{off} = 20$, 55, and 200 pN-sec/μm, respectively; red circles are experimental data points). E: Model predictions of mean-squared angular displacement versus time for three distances between the centrosome position and the nuclear centroid (solid lines, from upper to lower: black, 8 μm, blue, 3 μm, and red, 0.5 μm, respectively). [Color figure can be seen in the online version of this article, available at http://wileyonlinelibrary.com/journal/jcp]

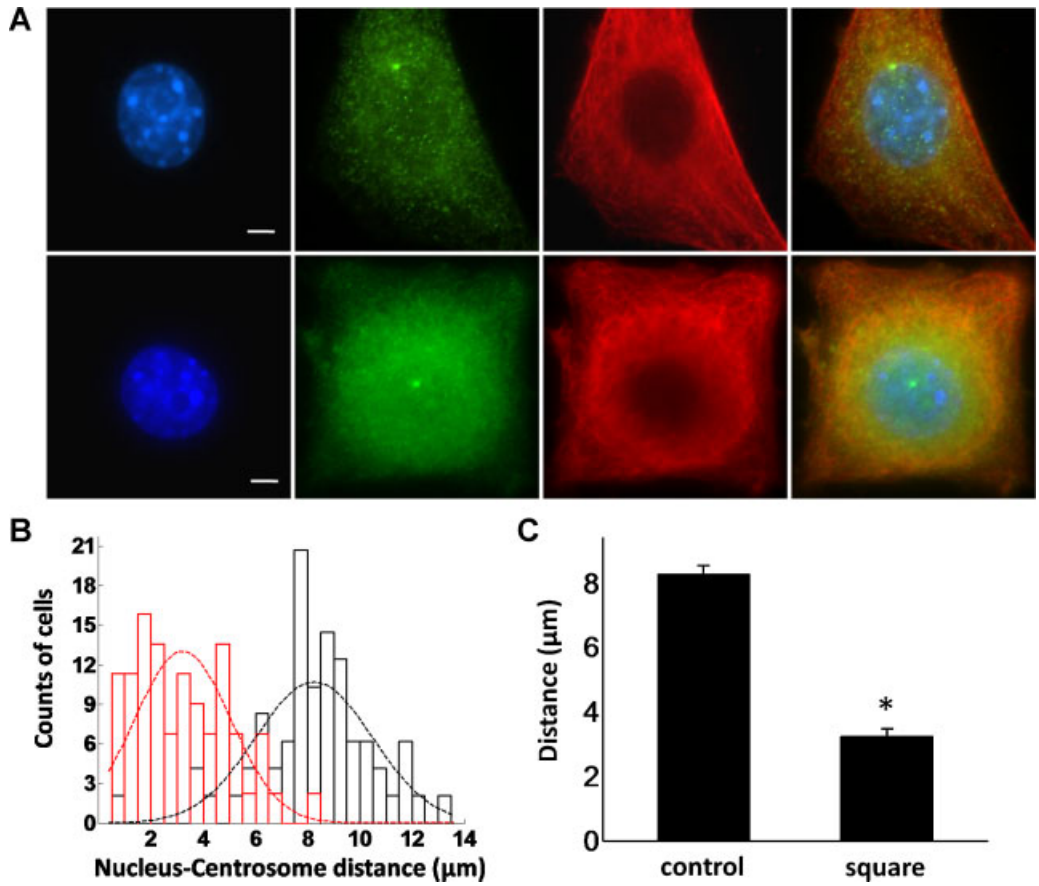

Fig. 5. Distance between the centrosome and the nucleus decreased in patterned square NIH 3T3 cells. A: Positions of the centrosome (green) in unpatterned (top part) and patterned cells (bottom part). Nucleus is stained blue and microtubules in red. The last two pictures on the right are overlay images. All scale bars are 5 μm. B: Distributions of nuclear-centrosomal distance in unpatterned (black) and patterned cells (red). C: Nuclear-centrosomal distance in patterned square cells is significantly smaller than that in unpatterned cells. Error bars indicate SE; $^{*}P < 0.01$. [Color figure can be seen in the online version of this article, available at http://wileyonlinelibrary.com/journal/jcp]

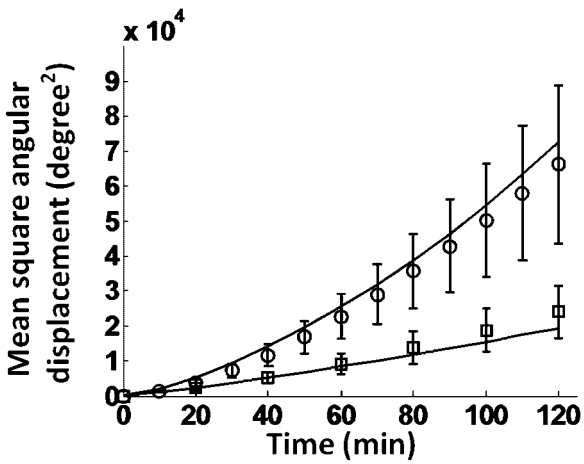

Fig. 6. Nuclear rotation in unpatterned cells (circles, n = 25) is significantly larger than that in patterned cells (squares, n = 24), which agrees with the MSD generated by simulation using experimentally measured average centrosome-nucleus distances of 8 and 3 μm, respectively (solid lines). Error bars indicate SE.

zero when the centrosome is positioned at the nuclear centroid because the radial position vector drawn from the centroid to the point of dynein forces becomes parallel to the microtubule (and mean dynein-force) direction (Fig. 3B). Also, the lever arm (the distance from the nuclear centroid to the MT–nucleus contact position) is smaller (Fig. 3B).

That the centrosome is essentially stationary during rotation is consistent with similar findings reported in two other studies (Levy and Holzbaur, 2008; Gerashchenko et al., 2009). Consistent with these findings, the model does not require the centrosome to rotate for the nucleus to rotate—rather, the origin of the torque is due to the asymmetric spatial distribution of nuclear associated microtubules. Thus, the centrosome is actually relevant to the rotation process because its position controls the degree of spatial asymmetry thereby influencing the rate of rotation.

The model qualitatively reproduces our experimental finding that nuclear rotation is a random walk with directional persistence. The fluctuations are a natural consequence of the fact that the microtubule configuration fluctuates due to dynamic instability. The time over which the nuclear rotation persists on average in a given direction is the time it takes for an initial asymmetry in the microtubule configuration to be reversed by dynamic instability. Thus, the model nicely explains a number of features of nuclear rotation that have been observed by us and other researchers.

The model assumes a linear force-speed relationship for dynein, similar to another recent paper on dynein mediated nuclear movement (Vogel et al., 2009). Given the level of coarse graining in the model, small deviations from linearity would not alter the main conclusions of the paper. Although Equation (1) allows a load on the motor in the (−)-end direction ($\mathbf{n}\cdot\mathbf{f} > 0$) to enhance the motor speed above v_{max}, because tangential speeds (~0.001 μm/sec) are much less than v_{max}, this situation is rarely encountered in the application of the model. Therefore, any nonlinearity in the "force-assisted" region of the force–velocity relation for dynein that is not accounted for in the model should not impact the model predictions.

Dynein pulling has been proposed previously as a mechanism for pulling of microtubule organizing centers (Burakov et al., 2003). A recent model for oscillatory spindle pole body translation in *S. pombe* assumed that directional translation arises from breakage of dynein linkages by the "winning" side in a tug-o-war of competing pulling microtubules (Vogel et al., 2009). In that model, the spindle body translates at nearly constant maximum motor speed until it reaches one end of the cell, consistent with the experimental observations in that system. In contrast, nucleus rotational speeds are stochastic, fluctuating in magnitude and direction, but with values much smaller than the dynein motor speed v_{max}, suggesting no winning side of the dynein tug-o-war. We also note that there is no direct experimental evidence of dynein-force-induced breakage of dynein linkages in vivo, and our model can explain the relevant observations without invoking this untested assumption. In fact, for observed maximum tangential speed of $S = 0.001$ μm/sec, the force over the bond lifetime (given by $S\kappa/k_{off}$) is significantly smaller than 1 pN for our estimates of κ/k_{off} (see model results). This force is much smaller than forces required for bond breakage that are typically several pN (Evans, 2001).

There is evidence that nuclear rotation can be influenced by other molecules. For example, Ji et al. (2007) showed that over-expression of nesprin-1, a protein that binds the nucleus to the F-actin cytoskeleton, reduces the extent of rotation. This suggests that rotation may at least in part be influenced by frictional drag due to connections with other members of the cytoskeleton. However, we did not observe an increase in the rotation in NIH3T3 fibroblasts on nesprin-1 depletion (Fig. S4). Similarly, myosin inhibition may increase rotation (Levy and Holzbaur, 2008), which again suggests a role for actomyosin in opposing the rotation. Drag in our model is due to dynein motors bound to those microtubules that oppose the rotation. We cannot rule out drag due to frictional connections with actin or intermediate filaments. While including this effect would add a term similar to the drag due to dynein, it is not expected to change the main conclusions of the model.

Acknowledgments

T.P.L. gratefully acknowledges support from NSF CMMI-0954302 and AHA-0735203N, and R.B.D. acknowledges support of NSF CTS-0505929.

Literature Cited

Albrecht-Buehler G. 1984. Movement of nucleus and centrosphere in 3T3 cells. In: Levine AJ, Woude GFV, Toop WC, Watson JD, editors. Cancer cells: The transformed phenotype. New York: Cold Spring Harbor Laboratory. pp 87–96.

Allen VW, Kropf DL. 1992. Nuclear rotation and lineage specification in Pelvetia embryos. Development 115, 873–883.

Brock AL, Ingber DE. 2005. Control of the direction of lamellipodia extension through changes in the balance between Rac and Rho activities. Mol Cell Biomech 2:135–143.

Burakov A, Nadezhdina E, Slepchenko B, Rodionov V. 2003. Centrosome positioning in interphase cells. J Cell Biol 162:963–969.

Chancellor TJ, Lee J, Thodeti CK, Lele T. 2010. Actomyosin tension exerted on the nucleus through nesprin-1 connections influences endothelial cell adhesion, migration, and cyclic strain-induced reorientation. Biophys J 99(1): 115–123.

Evans E. 2001. Probing the relation between force—lifetime—and chemistry in single molecular bonds. Annu Rev Biophys Biomol Struct 30:105–128.

Fink J, Thery M, Azioune A, Dupont R, Chatelain F, Bornens M, Piel M. 2007. Comparative study and improvement of current cell micro-patterning techniques. Lab Chip 7:672–680.

Fridolfsson HN, Ly N, Meyerzon M, Starr DA. 2010. UNC-83 coordinates kinesin-1 and dynein activities at the nuclear envelope during nuclear migration. Dev Biol 338:237–250.

Gennerich A, Carter AP, Reck-Peterson SL, Vale RD. 2007. Force-induced bidirectional stepping of cytoplasmic dynein. Cell 131:952–965.

Gerashchenko MV, Chernoivanenko IS, Moldaver MV, Minin AA. 2009. Dynein is a motor for nuclear rotation while vimentin IFs is a "brake." Cell Biol Int 33:1057–1064.

Gliksman NR, Skibbens RV, Salmon ED. 1993. How the transition frequencies of microtubule dynamic instability (nucleation, catastrophe, and rescue) regulate microtubule dynamics in interphase and mitosis: Analysis using a Monte Carlo computer simulation. Mol Biol Cell 4:1035–1050.

Gomes ER, Jani S, Gundersen GG. 2005. Nuclear movement regulated by Cdc42, MRCK, myosin, and actin flow establishes MTOC polarization in migrating cells. Cell 121:451–463.

Gros-Louis F, Dupre N, Dion P, Fox MA, Laurent S, Verreault S, Sanes JR, Bouchard JP, Rouleau GA. 2007. Mutations in SYNE1 lead to a newly discovered form of autosomal recessive cerebellar ataxia. Nat Genet 39:80–85.

Howard J. 2006. Elastic and damping forces generated by confined arrays of dynamic microtubules. Phys Biol 3:54–66.

Jaalouk DE, Lammerding J. 2009. Mechanotransduction gone awry. Nat Rev Mol Cell Biol 10:63–73.

Ji JY, Lee RT, Vergnes L, Fong LG, Stewart CL, Reue K, Young SG, Zhang Q, Shanahan CM, Lammerding J. 2007. Cell nuclei spin in the absence of lamin b1. J Biol Chem 282:20015–20026.

Khatau SB, Hale CM, Stewart-Hutchinson PJ, Patel MS, Stewart CL, Searson PC, Hodzic D, Wirtz D. 2009. A perinuclear actin cap regulates nuclear shape. Proc Natl Acad Sci USA 106:19017–19022.

King SJ, Brown CL, Maier KC, Quintyne NJ, Schroer TA. 2003. Analysis of the dynein–dynactin interaction in vitro and in vivo. Mol Biol Cell 14:5089–5097.

Lee JS, Chang MI, Tseng Y, Wirtz D. 2005. Cdc42 mediates nucleus movement and MTOC polarization in Swiss 3T3 fibroblasts under mechanical shear stress. Mol Biol Cell 16:871–880.

Levy JR, Holzbaur EL. 2008. Dynein drives nuclear rotation during forward progression of motile fibroblasts. J Cell Sci 121:3187–3195.

Morris NR. 2003. Nuclear positioning: The means is at the ends. Curr Opin Cell Biol 15:54–59.

Paddock SW, Albrecht-Buehler G. 1988. Rigidity of the nucleus during nuclear rotation in 3T3 cells. Exp Cell Res 175:409–413.

Parker KK, Brock AL, Brangwynne C, Mannix RJ, Wang N, Ostuni E, Geisse NA, Adams JC, Whitesides GM, Ingber DE. 2002. Directional control of lamellipodia extension by constraining cell shape and orienting cell tractional forces. FASEB J 16:1195–1204.

Pomerat CM. 1953. Rotating nuclei in tissue cultures of adult human nasal mucosa. Exp Cell Res 5:191–196.

Quintyne NJ, Gill SR, Eckley DM, Crego CL, Compton DA, Schroer TA. 1999. Dynactin is required for microtubule anchoring at centrosomes. J Cell Biol 147:321–334.

Russell RJ, Xia SL, Dickinson RB, Lele TP. 2009. Sarcomere mechanics in capillary endothelial cells. Biophys J 97:1578–1585.

Shelden E, Wadsworth P. 1993. Observation and quantification of individual microtubule behavior in vivo: Microtubule dynamics are cell-type specific. J Cell Biol 120:935–945.

Starr DA. 2009. A nuclear-envelope bridge positions nuclei and moves chromosomes. J Cell Sci 122:577–586.

Thery M, Racine V, Piel M, Pepin A, Dimitrov A, Chen Y, Sibarita JB, Bornens M. 2006. Anisotropy of cell adhesive microenvironment governs cell internal organization and orientation of polarity. Proc Natl Acad Sci USA 103:19771–19776.

Toba S, Watanabe TM, Yamaguchi-Okimoto L, Toyoshima YY, Higuchi H. 2006. Overlapping hand-over-hand mechanism of single molecular motility of cytoplasmic dynein. Proc Natl Acad Sci USA 103:5741–5745.

Vogel SK, Pavin N, Maghelli N, Julicher F, Tolic-Norrelykke IM. 2009. Self-organization of dynein motors generates meiotic nuclear oscillations. PLoS Biol 7:e1000087.

Wang N, Tytell JD, Ingber DE. 2009. Mechanotransduction at a distance: Mechanically coupling the extracellular matrix with the nucleus. Nat Rev Mol Cell Biol 10:75–82.

Warren DT, Zhang Q, Weissberg PL, Shanahan CM. 2005. Nesprins: Intracellular scaffolds that maintain cell architecture and coordinate cell function? Expert Rev Mol Med 7:1–15.

Yamada M, Toba S, Takitoh T, Yoshida Y, Mori D, Nakamura T, Iwane AH, Yanagida T, Imai H, Yu-Lee LY, Schroer T, Wynshaw-Boris A, Hirotsune S. 2010. mNUDC is required for plus-end-directed transport of cytoplasmic dynein and dynactins by kinesin-1. EMBO J 29:517–531.

Yao KT, Ellingson DJ. 1969. Observations on nuclear rotation and oscillation in Chinese hamster germinal cells in vitro. Exp Cell Res 55:39–42.

Zhang X, Xu R, Zhu B, Yang X, Ding X, Duan S, Xu T, Zhuang Y, Han M. 2007. Syne-1 and Syne-2 play crucial roles in myonuclear anchorage and motor neuron innervation. Development 134:901–908.

Zhou K, Rolls MM, Hall DH, Malone CJ, Hanna-Rose W. 2009. A ZYG-12-dynein interaction at the nuclear envelope defines cytoskeletal architecture in the *C. elegans* gonad. J Cell Biol 186:229–241.